THE JET/ISM INTERACTION IN THREE NEARBY RADIO GALAXIES AS SEEN WITH *CHANDRA*

R. P. Kraft
Harvard/Smithsonian Center for Astrophysics
60 Garden St., MS-67, Cambridge, MA 02138
RKRAFT@CFA.HARVARD.EDU
W. R. Forman, E. C. Churazov, J. Eilek, M. J. Hardcastle, S. Heinz, C. Jones, M. Markevitch, S. S. Murray, P. E. J. Nulsen, F. Owen, A. Vikhlinin, D. M. Worrall
WFORMAN@CFA.HARVARD.EDU, CHURAZOV@MPA-GARCHING.MPG.DE, JEILEK@AOC.NRAO.EDU
M.HARDCASTLE@BRISTOL.AC.UK, HEINZS@SPACE.MIT.EDU, CJONES@CFA.HARVARD.EDU
MMARKEVITCH@CFA.HARVARD.EDU, SSM@CFA.HARVARD.EDU, PNULSEN@CFA.HARVARD.EDU,
FOWEN@AOC.NRAO.EDU, AVIKHLININ@CFA.HARVARD.EDU, D.WORRALL@BRISTOL.AC.UK

Abstract

Chandra observations of radio galaxies have demonstrated a wide range of complex interactions between their jets and the ambient interstellar/intracluster medium (ISM/ICM). In this paper, we discuss results from *Chandra* observations of jet/ISM interactions in three nearby radio galaxies: Centaurus A (3.4 Mpc), M87 (16 Mpc), and NGC507 (66.7 Mpc). We present observational details for each object, and discuss how these relate to the more general picture of jet/ISM interactions. In Centaurus A, we have detected a hot, dense shell of gas surrounding the southwest radio lobe that we attribute to the supersonic expansion of the lobe into the ISM. There is some evidence of a similar interaction around the northeast radio lobe, although two orders of magnitude less X-ray luminous. We discuss the implications of this shell and the asymmetry. A deep *Chandra* observation (100 ks) of M87 indicates complex structures over a range of scales. Features include several X-ray cavities related to the radio cocoon in the central $45''$, an X-ray cavity coincident with a radio feature that lies perpendicular to the jet/counter jet axis suggestive of a buoyant bubble, and several roughly concentric surface brightness discontinuities in the larger scale gas indicative of shocks produced by multiple radio outbursts. *Chandra* observations of NGC507 have detected a large surface brightness discontinuity related to the expansion of the radio lobes. The temperature difference across the discontinuity is small ($\sim 10\%$), so that this is not a 'cold-front' of the type that has been commonly seen by *Chandra* in cluster mergers. The appearance of this feature is most likely due to the entrainment of higher abundance gas from the central regions of the galaxy as the lobe expands at roughly the sound speed of the ambient gas.

1 Introduction

The study of jets, whether terrestrial or astrophysical, requires knowledge of the properties of the collimated flow and of the medium into which it is propagating. Our understanding of astrophysical jets has made great steps forward since the launch of *Chandra* and *XMM-Newton* in 1999; these observations have permitted us to study with unprecedented sensitivity the non-thermal X-ray emission from jet knots and lobe hot spots, as well as the hot, X-ray emitting gas into which these jets are propagating. Prior to the launch of these X-ray observatories, non-thermal X-ray emission had been detected from only a handful of extragalactic jets (e.g., Cen A, M87, and 3C273). Now there are dozens of jets from which X-ray emission has been detected. Likewise, evidence of jet - intracluster medium (jet/ICM) interactions with the ambient medium had only been observed in a small number of bright, nearby objects (e.g., Per A, Cyg A) prior to the *Chandra* and *XMM-Newton* era. This phenomenon has now been observed in dozens of clusters, groups, and individual galaxies.

A wide variety of structures have been observed in the X-ray emitting coronae surrounding radio galaxies. Echoes of multiple nuclear outbursts have been observed in the corona of Perseus A (Fabian et al., 2003). Evacuated cavities, sometimes bordered by cool shells, have been seen in the ICM of several galaxies including M84 (Finoguenov & Jones, 2000), NGC4636 (Jones et al., 2002), 3C317 (Blanton et al., 2001), Hydra A (McNamara et al., 2000), and PKS 2354−35 (Heinz et al., 2002). In most of these cases, evidence of strong shocks is not seen. If the inflation of the radio lobes is subsonic, the energy can be transferred to the gas either by weak shocks as a result of inflation of the lobes and/or subsequently by dissipative processes such as turbulent entrainment as the bubble rises buoyantly. Subsonic motions of radio lobes can play an important role in the dynamics and energetics of the ICM (Croston, 2005). The study of the jet/ICM interaction has generated wider interest recently because of the realization that the large amount of cool (< 0.5 keV) gas in cluster cooling flows predicted on the basis of observations with the previous generation of X-ray observatories does not, in fact, exist (Peterson et al., 2001; Sakelliou et al., 2002; Xu et al., 2002). Since the radiative cooling time of the gas in the central regions of dense clusters is a small fraction of the Hubble time, radiative losses in cluster (and galaxy) cores must be balanced by energy input from another source. Two potential mechanisms currently in vogue that can supply the necessary energy are thermal conduction from the gas reservoir at large radii and central heating from active galactic nuclei (AGN) outbursts.

In this paper, we briefly summarize X-ray and radio observations of three nearby radio galaxies: Cen A, M87, and NGC507. The focus of this paper is on the relationship between the AGN outflows, seen as jets and radio lobes, and the X-ray emitting coronae.

2 Radio galaxy - interstellar medium interactions

2.1 Centaurus A

Centaurus A is the nearest (d = 3.4 Mpc, $1'' = 17$ pc; Israel (1998)) radio galaxy to the Milky Way. It is commonly classified as an FRI galaxy based on its radio luminosity and structure, although it is morphologically very different from canonical FRIs such as 3C31 and 3C449. An adaptively smoothed *Chandra* ACIS-I X-ray image of Cen A ($\sim$ 72 ks) in the 1–3 keV band

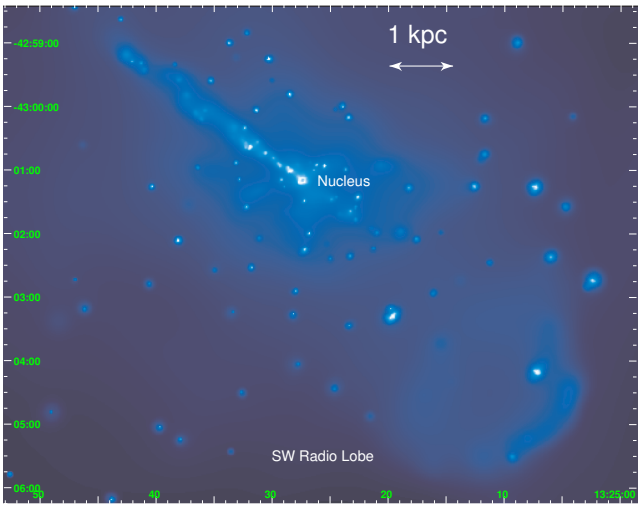

Figure 1: Adaptively smoothed *Chandra* ACIS-I image of Centaurus A in the 1.0–3.0 keV band. The bright active nucleus is at the center of the image, the X-ray jet extends $\sim 4'$ to the northeast. Hundreds of X-ray binaries can also be seen. Note the region of diffuse emission to the southwest of the nucleus and the bright enhancement at the edge of this region $\sim 6'$ from the nucleus. We model this region as a hot, shock-heated shell of gas surrounding the radio lobe that was created by the supersonic expansion/inflation of the lobe into the ISM.

is shown in Fig. 1. The multi-component X-ray emission is apparent, with hundreds of low-mass X-ray binaries, the jet to the northeast and the bright active nucleus in the center of the image. Detailed discussion of the X-ray and radio emission from the jet is presented elsewhere (Kraft et al., 2002; Hardcastle et al., 2003, 2005). Perhaps the most striking feature in Fig. 1, however, is the diffuse emission to the southwest coincident with the southwest radio lobe. An X-ray image of this region with 13 cm radio contours overlaid is shown in Fig. 2.

Based primarily on energetics, spectra, and morphological differences between the X-ray and radio images, we reject a non-thermal origin for this emission and conclude that this is a cap or half a shell of material swept up by the supersonic expansion of the radio lobe into the ambient medium (Kraft et al., 2003; Worrall et al., 2005). The resolution of the 13 cm radio data shown in Fig. 2 is lower ($30'' \times 20''$ beam) than the smooth X-ray image. This, combined with the effects of projection, implies that the X-ray enhancement along the edge of the southwest radio lobe is actually beyond or exterior to the lobe. The temperature of the shell is ~ 2.9 keV, and the temperature of the ambient

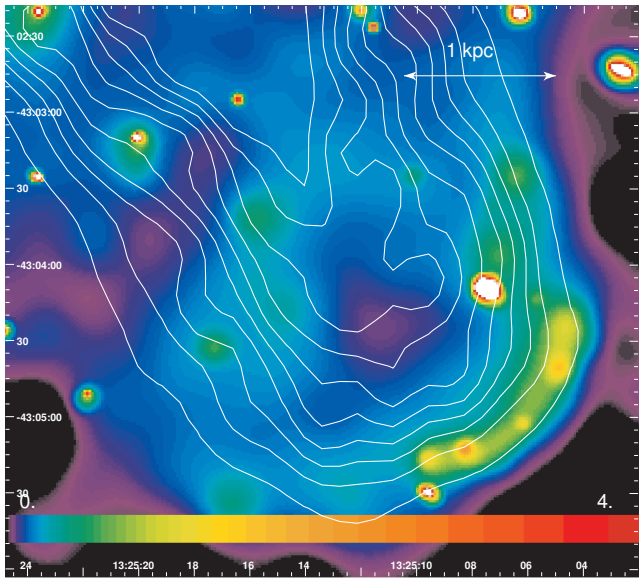

Figure 2: Adaptively smoothed *Chandra* ACIS-I image of the southwest radio lobe in the 0.5–2.0 keV band with 13 cm (ATCA - $30'' \times 20''$ beam) radio contours overlaid.

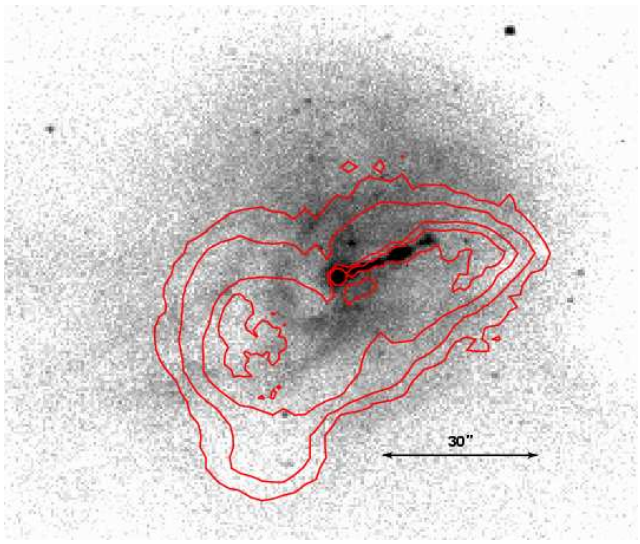

Figure 3: Unsmoothed *Chandra* ACIS-S X-ray image in the 0.5–2.0 keV band of the central region of M87 with 6 cm radio contours overlaid (Hines et al., 1989). Note the correspondence of the radio lobes to the east of the nucleus with the X-ray cavities.

ISM is $\sim$ 0.29 keV. Based on the pressure difference between the shell and the ambient medium, we estimate the expansion velocity to be $\sim$ 2400 km s^{-1}, or roughly Mach 8 relative to the ambient medium. The X-ray morphology of the shell, the sharpness of the shock front, and the thickness of the shell relative to the size of the radio lobe, are all qualitatively consistent with this high Mach number.

This result has several important implications. First, it runs counter to the conventional paradigm that the lobes of FRI galaxies are expanding subsonically, although as stated above, Cen A is morphologically very different from 'canonical' FRI radio galaxies such as the 'twin tailed jet' 3C31 (Leahy, 1993). Second, the pressure of this cap is an order of magnitude larger than the equipartition pressure estimated from multi-frequency radio observations (Feigelson et al., 1981). This implies that the equipartition pressure considerably underestimates the true pressure; otherwise the shock heated shell would crush the lobe in a sound crossing time. The pressure of the lobe must be dominated by unseen low energy relativistic electrons, cold protons, or magnetic fields. Third, the thermal energy in the shell is $\sim 4\times10^{55}$ erg, which is a substantial fraction of the thermal energy of the hot ISM, $\sim 2\times10^{56}$ erg, within 15 kpc of the nucleus. It is by no means clear that all of this energy in the shell will eventually be converted to thermal energy of the ISM, but there is sufficient energy present to reheat any galaxy scale cooling flow.

2.2 M87

M87 is the central galaxy of the nearby Virgo cluster (d = 16 Mpc, $1' = 4.65$ kpc). The complex X-ray structure of this object as seen in *ROSAT*, *XMM-Newton*, and *Chandra* observations has been reported in several papers (Böhringer et al., 1995; Churazov et al., 2002; Belsole et al., 2001; Young et al., 2002). M87 is the central galaxy of a classic cooling flow cluster. Based on radio observations (Owen et al., 2000; Binney, 1999), it has been argued that the mechanical power provided by the AGN outflow inferred from radio jets and lobe structures is more than sufficient to balance radiative energy losses and suppress the cooling flow. This result has taken on more importance recently in light of the more general *XMM-Newton* RGS and *Chandra* non-detections of the spectral signatures of cooling gas in cooling flows as described in the introduction.

A more recent, deeper (100 ks) *Chandra* ACIS-S observation of M87 shows several structures in the hot gas around M87 not previously reported (Forman et al., 2004). An X-ray image from this deep observation in the 0.5–2.0 keV band of the central region of M87 with radio contours overlaid is shown in Fig. 3.

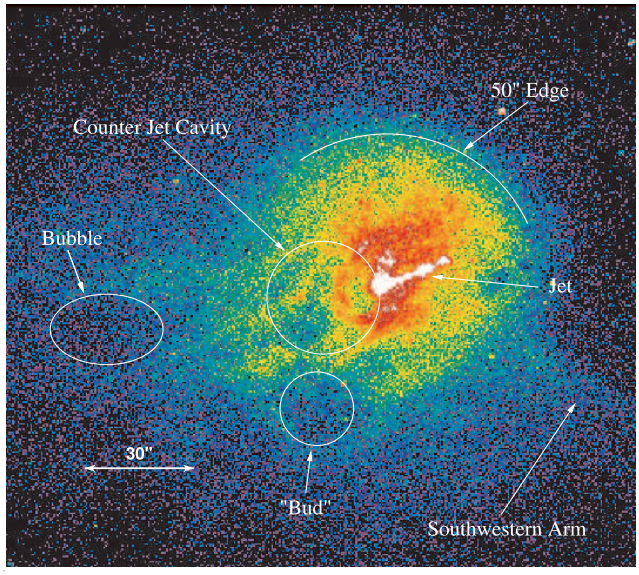

Figure 4: *Chandra* ACIS-S X-ray image in the 0.5–2.0 keV band of the central region of M87 in false color with various structures of interest labeled. See text for complete description.

The active nucleus is at the center of the image, and the well-known jet extends to the NW. The jet makes a small angle to the line of sight ($\sim 20°$; Biretta et al. (1999)), so that the radio lobe seen surrounding the jet and the lobe in the counter jet direction are considerably larger than seen in projection. The X-ray emitting gas is clearly not azimuthally symmetric around the nucleus. The radio lobes are surrounded by an elliptical X-ray cavity. To the east of the nucleus, there are several cavities coincident with the peak of the radio emission, and several smaller cavities beyond the radio lobe surrounded by filamentary structure. There is evidence of a surface brightness discontinuity, most prominent to the north, that may be a result of weak shocks driven by nuclear activity (Young et al., 2002). Some of the structure in the central region may be the result of thermal conduction between the hot gas and cooler clouds (Sparks et al., 2004). All of these features are more clearly identified and labeled in Fig. 4.

Larger scale X-ray structures are shown in Fig. 5. To enhance the visual appearance of low surface brightness features, the same data are shown in Fig. 6 with the azimuthal average surface brightness subtracted. Several structures are seen including the bifurcation of the eastern and southwestern arms, and three surface brightness discontinuities (at $3'$ (14 kpc), $3.75'$ (17 kpc), and $8'$ (37 kpc) from the nucleus) indicative of multiple nuclear outbursts. An *XMM-Newton* MOS temperature map with 90 cm radio contours overlaid is shown in Fig. 7. The temperature of the arms is less than that of the ambient gas and consistent with that at the center of M87 (Molendi, 2002), suggesting that the colder material from the center has been entrained and uplifted by the motion of the radio components. We briefly describe two of the more interesting features of M87 below, the surface brightness discontinuities and the 'budding' bubble.

2.2.1 Surface brightness discontinuities - azimuthal rings

We detect three sharp surface brightness discontinuities at distances of $3'$ (14 kpc), $3.75'$ (17 kpc), and $8'$ (37 kpc) (see also Young et al. (2002)). The first two are most visible to the north and west of the nucleus, and the third to the southwest (see Fig. 6). The remarkable spherical symmetry of these features strongly suggests that they are related to nuclear events. We attribute all of these features to multiple AGN outbursts where the supersonic expansion of the radio lobes drove strong shocks into the ISM. The inflation of the radio lobes was initially supersonic, but in each case decelerated as the lobe inflated, ultimately to be driven by buoyancy forces. The discontinuities are the 'remnant' of this early supersonic phase in each outburst. Contrast this with Cen A above which is currently in the supersonic phase. The shock heated gas is visible in front of the expanding/inflating radio lobe.

To estimate the energy of the most recent outburst, we have determined the deprojected gas temperature and density profile across the $3'$ discontinuity, and compared this to a model in which all of the energy is deposited as a single event by the AGN and propagates outward as a spherically symmetric shock. We assume that the atmosphere is isothermal and in hydrostatic equilibrium, and that the density distribution is described by a power-law determined from the surface brightness profile beyond the shock. The model that best matches the data is one in which 8×10^{57} erg was deposited in the gas $\sim 10^7$ years ago. The shock is only mildly supersonic ($\mathcal{M}$ = 1.2, v = 950 km s^{-1}). The enthalpy of the gas displaced by the inner radio lobes, an upper limit to the work done on the gas by the subsonic inflation of the lobes, is approximately three times less than the energy in the shock. The power of the shock averaged over 10^7 years is $\sim 2.4\times10^{43}$ erg

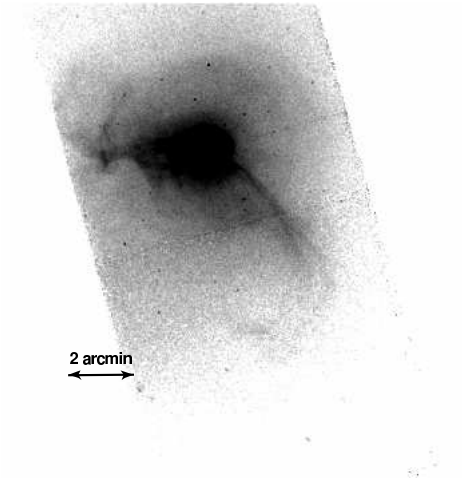

Figure 5: Smoothed, exposure corrected *Chandra* ACIS-S image of M87 in the 0.5–2.0 keV band. The eastern and southwestern arms are visible, as is the surface brightness discontinuity $\sim 3'$ from the nucleus.

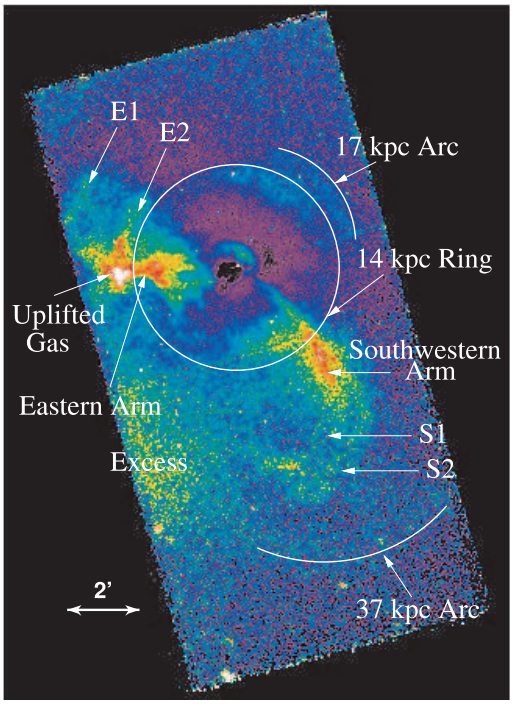

Figure 6: Smoothed, exposure corrected *Chandra* ACIS-S image of M87 in the 0.5–2.0 keV band with the azimuthally averaged profile subtracted to enhance the appearance of low surface brightness features. Several interesting structures are seen including the bifurcation of the eastern and southwestern arms, and three surface brightness discontinuities (at $3'$, $3.75'$, and $8'$ from the nucleus) indicative of multiple nuclear outbursts. The extensions of the eastern and southwestern arms after they divide have been labeled E1/2 and S1/2, respectively.

s^{-1}, a factor of a few greater than the radiative losses ($\sim 10^{43}$ erg s^{-1}; Stewart et al. (1984)) of the cooling flow. This suggests that shocks are the most important means of transferring the mechanical energy of the AGN outburst into thermal energy of the ambient gas and balancing radiative losses. The 17 kpc surface brightness discontinuity is a relic of an earlier nuclear outburst. If the disturbance producing the second enhancement ($3.75'$) is traveling at the sound speed of the gas, it must have occurred $\sim 4\times10^6$ years before the outburst responsible for the 14 kpc ring. The third discontinuity ($8'$) lies just beyond the largest scale radio features which are believed to be the oldest (10^8 yrs) structures in M87 (Owen et al., 2000).

2.2.2 Budding bubble

It is typically assumed that the outflow from the nucleus is axial. In the majority of radio galaxies, jet/lobe structures are generally aligned in opposing directions from the nucleus (ignoring such phenomenon as wide-angle tailed sources and narrow-angle tailed sources that are believed to be the result of bulk motions, perhaps irregular, of the central galaxy relative to the larger scale environment, although buoyancy forces may be important as well (Worrall et al., 1995). Most of the X-ray and radio structures of the inner region of M87 are generally aligned with the jet/counter-jet direction; however, there is a limb brightened X-ray cavity coincident with a radio bubble to the south of the radio lobe in the counter-jet direction. This feature (labeled 'bud' in Fig. 4) is a 'budding' bubble that has broken off from the radio lobe and is now rising buoyantly in the cluster gas. The X-ray emission traces the boundary of the cavity filled with relativistic plasma (see Fig. 3. We speculate the separation of this 'budding' bubble may indicate a region of weakened magnetic field. If we assume that the bubble is buoyant and limited by the drag of the ICM, we estimate the rise time of the bubble to be $\sim 10^7$ years. It is therefore most likely associated with the current nuclear outburst.

2.3 NGC507

NGC507 is the central galaxy of the nearby Pisces cluster (d = 66.7 Mpc, $1'$ = 19.6 kpc). This is one of the most X-ray luminous early-type galaxies in the local universe ($L_x \sim 10^{43}$ erg s^{-1}), and *ROSAT* observations suggested that there was a large cooling flow (cooling

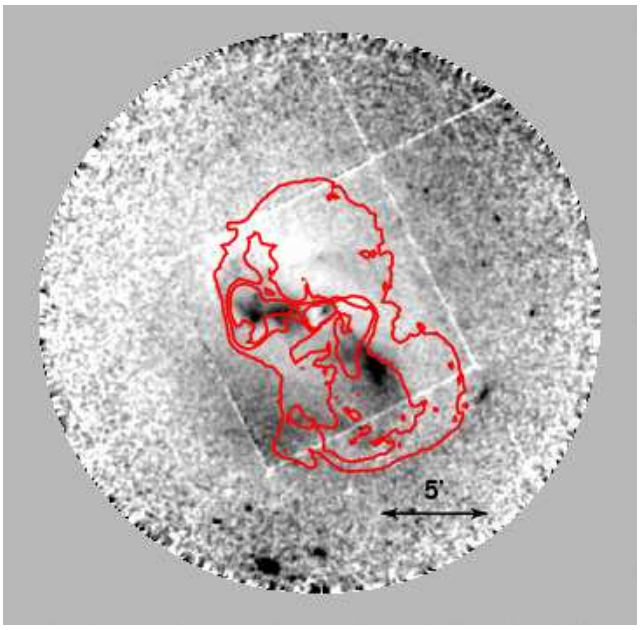

Figure 7: An *XMM-Newton* MOS temperature map with 90 cm radio contours overlaid. The eastern and southwestern arms are both cooler than the surrounding gas (Belsole et al., 2001; Molendi, 2002) suggesting that they are the result of entrainment of material from the central region.

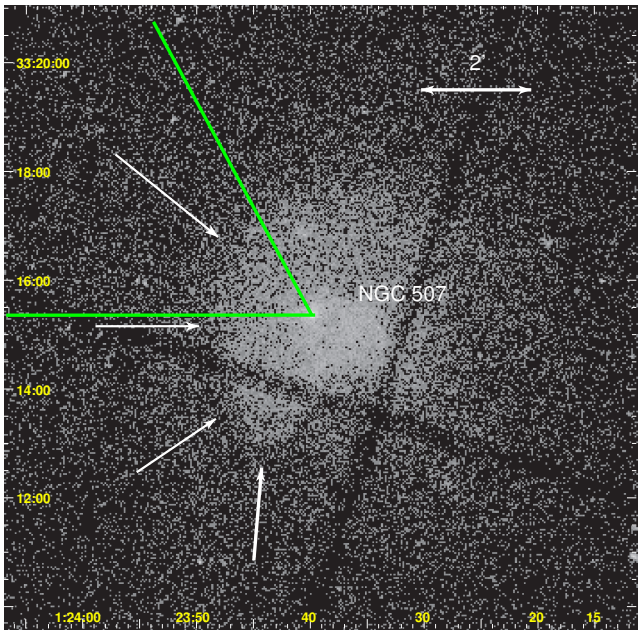

Figure 8: *Chandra* ACIS-I image of NGC507 in the 0.5–2.0 keV band. The white arrows delineate the sharp surface brightness discontinuity described in the text. The green sector denotes the region used for the spectral analysis presented in Fig. 9 and the surface brightness profile in Fig. 11.

rate of 30-40 $M_\odot$ yr^{-1}) at the center (Kim & Fabbiano, 1995; Paolillo et al., 2003). NGC507 contains an FRI radio galaxy (Fanti et al., 1986), and is listed in the B2 catalog. An unsmoothed *Chandra* ACIS-I image of this galaxy is shown in Fig. 8. NGC507 is located at the vertex of the green sector shown in the image. Details of this observation have been published in Kraft et al. (2004).

One of the most striking features of the X-ray image in Fig. 8 is the sharp surface brightness discontinuity (delineated by the white arrows) extending 120° from the northeast to the southeast of the galaxy. An adaptively smoothed X-ray image with two different sets of radio contours overlaid (both at 1.4 GHz, but different beams) is shown in Fig. 9. Note the correspondence between the outer NVSS[1] radio contour and the X-ray surface brightness discontinuity. This suggests that the discontinuity has been created by the expansion/inflation of the radio lobe.

The temperature and elemental abundance in six annular regions of the green sector of Fig. 8 is plotted in Fig. 10. Interestingly, there is almost no temperature difference across the discontinuity. This is in sharp contrast to the cluster 'cold fronts' often seen in *Chandra* observations of merging clusters (Vikhlinin et al., 1999, 2001). A temperature map indicates that the coldest gas is located along the discontinuity to the south/southwest of NGC507. The temperature of this gas is only about $\sim$ 15% cooler than the gas on the other side of the discontinuity. The surface brightness discontinuity is not a 'cold front', and must therefore either be related to a discontinuity in the density of the gas or the emissivity (i.e., abundance) of the gas. If the surface brightness discontinuity is caused by a large discontinuity in density alone (shown as Model #1 in Fig. 11), this would imply a sharp pressure discontinuity as well. There is no evidence of a hot shell of gas around the discontinuity, so that the expansion velocity must only be mildly supersonic ($\mathcal{M} < 1.2$) or subsonic. The discontinuity is extremely sharp, however, and if the expansion velocity is subsonic or even mildly supersonic, it is difficult to understand how such a sharp pressure and density discontinuity formed or is maintained. At such relatively low velocities, there should be a small jump in density across the shock front, and a gradual increase in density between the shock front and the stagnation point, which should be well sepa-

[1]National Radio Astronomy Observatory (NRAO) Very Large Array (VLA) Sky Survey (Condon et al., 1998)

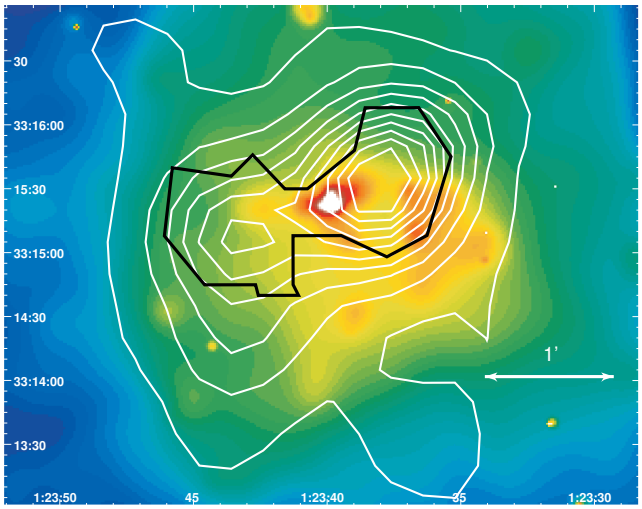

Figure 9: Adaptively smoothed X-ray image (0.5–2.0 keV) band with NVSS (white - 1.4 GHz (Condon et al., 1998)) and higher resolution (black - 1.4 GHz (de Ruiter et al., 1986)) VLA radio contours overlaid. Notice the correlation between the outer NVSS contour and the discontinuity.

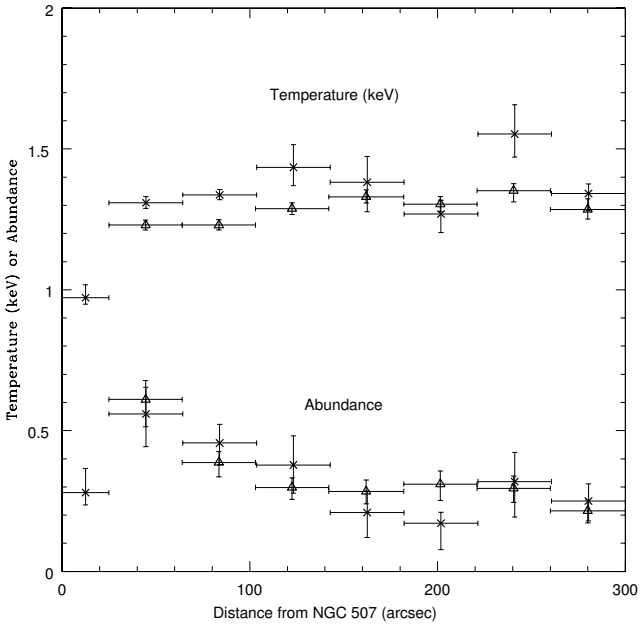

Figure 10: The temperature (top set of points) and the elemental abundance (bottom set of points) in six annular regions of the green sector shown in Fig. 8. The triangles and the squares correspond to *Chandra* and *XMM-Newton* MOS data, respectively.

rated spatially.

As an alternative, we propose a model in which there is a sharp discontinuity in the elemental abundance, and therefore emissivity, of the gas across this discontinuity. We assume the elemental abundance interior to the discontinuity is equal to the maximum given in Fig. 10 and that there is no pressure discontinuity so that the small temperature difference is balanced by a difference in density. The surface brightness of such a model is shown in Fig. 11 as Model #2. Such a sharp discontinuity could be created by entrainment of material with high elemental abundance from the galaxy center as the lobe inflates (Churazov et al., 2002). A sharp abundance discontinuity is not definitively seen in our data. The abundance appears to increase more gradually toward the center. We mention that a different analysis of the same data found a generally higher elemental abundance (Kim et al., 2004) than we quote here. We assumed that these features lie in the plane of the sky. If they are at a relatively small angle to the line of sight, the inferred pressure discontinuity would be larger as they would be further out in the halo. We have also modeled the gas as having uniform density interior to the discontinuity, although the results are not significantly different for any reasonable parameterization of the density distribution (e.g., a power law or β-model). This result suggests that the outflow of the radio lobe is a very efficient mechanism for transporting, and perhaps mixing, the high abundance material at the center of the galaxy with the lower abundance material in the halo.

3 Summary and conclusions

We have presented results from X-ray and radio observations of three nearby radio galaxies with very different structures. The conventional paradigm suggests that at the earliest stages of an AGN outburst, the 'lobes' are greatly overpressurized relative to the ambient medium and are highly supersonic, but as they inflate to kpc or tens of kpc scales, they rapidly decelerate and become subsonic, ultimately being driven by buoyancy forces. The 'gentle', subsonic motions of radio lobes on larger (kpc to tens of kpc scales) in dense environments have now been studied in more than a dozen cases with *Chandra* (Bîrzan et al., 2004). In dense environments, it is likely that we will only see the echo of this early, highly supersonic phase, as is the case for M87. The phase when the lobes are expanding at large Mach numbers is short-lived (Heinz & Enßlin , 2004). Shocks may be the most efficient means for AGN outflows to transfer their mechanical energy to the ambient medium and suppress cooling flows. To better understand the dynamics of this phe-

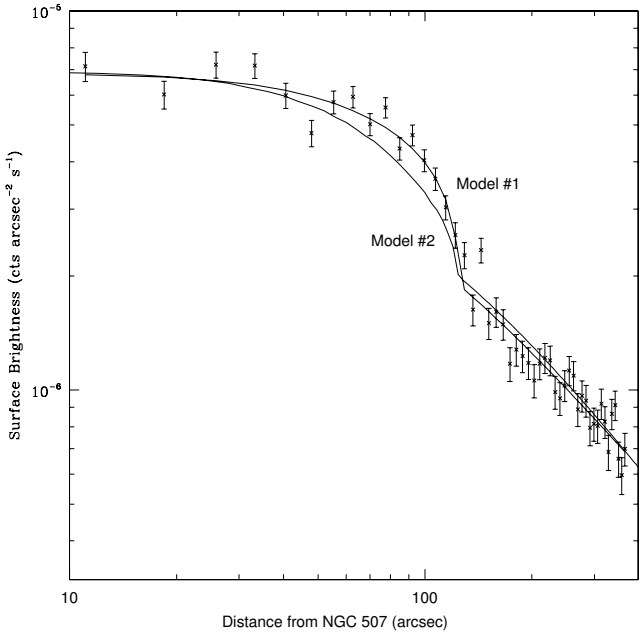

Figure 11: Surface brightness profile across the discontinuity in the green sector of Fig. 8. The curve labeled Model #1 corresponds to the best-fit model in which the density is discontinuous across the boundary. The density jump is more than a factor of two larger than the temperature difference, implying a large, unphysical pressure discontinuity. The other curve (Model #2 - the 'abundance front') corresponds to a model with a discontinuous jump in the elemental abundance across the discontinuity, but no jump in pressure.

nomenon and the importance of shocks in transferring energy, we must observe more examples in this supersonic phase. For radio galaxies in less dense environments (e.g., Cen A), the lobes will remain supersonic longer, the time scales will be shorter, and the length scales larger. The effect of a powerful AGN outburst in a poor environment is likely to be more dramatic as even a relatively small amount of heating may provide enough energy to the gas to blow the atmosphere off. This may ultimately be the solution to the long-standing puzzle of why the X-ray luminosities of early galaxies exhibit a large variance for a given optical luminosity. If there were a recent AGN outburst, the atmosphere could have been heated and may have escaped from the dark matter potential. Deeper *Chandra* and *XMM-Newton* observations of radio galaxies in poor environments will prove invaluable for understanding this phenomenon.

4 Acknowledgments

This work has been supported by NASA contracts NAS8-38248 and NAS8-39073. We would like to thank both the Local Organizing Committee and the Scientific Organizing Committee for their efforts in making this conference a success.

References

Belsole, E., et al. 2001, A&A, 365, L188.
Binney, J. 1999, in "Proceedings of the Ringberg Castle Workshop", 15-19 September 1997 (eds. Roser, Meisenheimer), Springer (New York), 116.
Biretta, J., Sparks, W., Macchetto, F. 1999, ApJ, 520, 621.
Bîrzan, L., Rafferty, D. A., McNamara, B. R., Wise, M. W., Nulsen, P. E. J. 2004, ApJ, 607, 800
Blanton, E. L., Sarazin, C. L., McNamara, B. R., Wise, M. W. 2001, ApJ, 558, L15.
Böhringer, H., Nulsen, P. E. J., Braun, R., Fabian, A. C. 1995, MNRAS, 274, L67.
Churazov, E., Sunyaev, R., Forman, W., Böhringer, H. 2002, MNRAS, 332, 729.
Condon, J. J., et al. 1998, AJ, 115, 1693.
Croston, J. H. 2005, these proceedings.
de Ruiter, H. R., Parma, P., Fanti, C., Fanti, R. 1986, A&A Suppl., 65, 111.
Fabian, A. C., Sanders, J. S., Crawford, C. S., Conselice, C. J., Gallagher, J. S., Wyse, R. F. G. 2003, MNRAS, 344, L48.
Fanti, C., Fanti, R., de Ruiter, H. R., Parma, P. 1986, A&A Suppl., 65, 145.
Feigelson, E. D., Schreier, E. J., Delvaille, J. P., Giacconi, R., Grindlay, J. E., Lightman, A. P. 1981, ApJ, 251, 31.
Finoguenov, A., Jones C. 2000, ApJ, 539, 603.
Forman, W. R., et al. 2004, ApJ, in press.
Hardcastle, M. J., Worrall, D. M., Kraft, R. P., Forman, W. R., Jones, C., Murray, S. S. 2003, ApJ, 593, 169.
Hardcastle, M. J. 2005, these proceedings.
Heinz, S., Choi, Y-Y., Reynolds, C. S., Begelman, M. C. 2002, ApJ, 569, L79.
Heinz, S., Enßlin, T. 2004, in "The Riddle of Cooling Flows in Galaxies and Clusters of Galaxies", eds. T. Reiprich, J. Kempner, N. Soker.
Hines, D., Owen, F., Eilek, J. 1989, ApJ, 347, 713.
Israel, F. P. 1998, Astron. Astrophys. Rev., 8, 237.
Jones, C., et al. 2002, ApJ, 567, L115.
Kim, D.-W., Fabbiano, G. 1995, ApJ, 441, 182.

Kim, D.-W., et al. 2004, ApJ, submitted.
Kraft, R. P., Forman, W. R., Jones, C., Murray, S. S., Hardcastle, M. J., Worrall, D. M. 2002, ApJ, 569, 54.
Kraft, R. P., et al. 2003, ApJ, 592, 129
Kraft, R. P., et al. 2004, ApJ, 601, 221
Leahy, P. 1993, in "Jets in Extragalactic Radio Sources", eds. Röser, H.-J., Meisenheimer, K., Berlin: Springer-Verlag.
McNamara, B. R., et al. 2000, ApJ, 534, L135.
Molendi, S. 2002, ApJ, 580, 815.
Owen, F., Eilek, J., Kassim, N. 2000, ApJ, 543, 611.
Paolillo, M., Fabbiano, G., Peres, G., Kim, D.-W. 2003, ApJ, 586, 850.
Peterson, J. R., et al. 2001, A.&A., 365, L104.
Sakelliou, I., et al. 2002, A.&A., 391, 903.
Sparks, W. B., Donahue, M., Jordán, A., Ferrarese, L., Ct, P. 2004, ApJ, 607, 294
Stewart, G. C., Fabian, A. C., Nulsen, P. E. J., Canizares, C. R. 1984, ApJ, 278, 536.
Vikhlinin, A., et al. 1999, ApJ, 520, L1.
Vikhlinin, A., Markevitch, M., Murray, S. S. 2001, ApJ, 551, 160.
Worrall, D. M., et al. 2005, these proceedings.
Worrall, D. M., Birkinshaw, M., Cameron, R. A. 1995, ApJ, 449, 93.
Xu, H., et al. 2002, ApJ, 579, 600.
Young, A. J., Wilson, A. S., Mundell, C. G. 2002, ApJ, 579, 560.